

Advances in Complex Systems
© World Scientific Publishing Company

Statistically validated lead-lag networks and inventory prediction in the foreign exchange market

DAMIEN CHALLET

*Laboratoire MICS, CentraleSupélec, Université Paris Saclay, 91190 Gif-sur-Yvette, France
and Enclade Capital SA, EPFL Innovation Park, Building C, 1015 Lausanne, Switzerland
damien.challet@centralesupelec.fr*

RÉMY CHICHEPORTICHE

Capital Fund Management, 23, rue de l'Université, 75007 Paris, France

MEHDI LALLOUACHE

BNP Paribas, 20, boulevard des Italiens, 75009 Paris, France

SERGE KASSIBRAKIS

Swissquote Bank SA, chemin de la Crétaux 33, 1196 Gland, Switzerland

Received (received date)

Revised (revised date)

We introduce a method to infer lead-lag networks of agents' actions in complex systems. These networks open the way to both microscopic and macroscopic states prediction in such systems. We apply this method to trader-resolved data in the foreign exchange market. We show that these networks are remarkably persistent, which explains why and how order flow prediction is possible from trader-resolved data. In addition, if traders' actions depend on past prices, the evolution of the average price paid by traders may also be predictable. Using random forests, we verify that the predictability of both the sign of order flow and the direction of average transaction price is strong for retail investors at an hourly time scale, which is of great relevance to brokers and order matching engines. Finally, we argue that the existence of trader lead-lag networks explains in a self-referential way why a given trader becomes active, which is in line with the fact that most trading activity has an endogenous origin.

Keywords: lead-lag networks; trader-resolved data; foreign exchange; prediction; inventory management.

1. Introduction

Predicting the evolution of complex systems is of great practical interest but difficult given their nonlinear collective dynamics and, in practice, *a priori* unknown networks of interaction between their elements (see e.g. [29, 36]). Determining the underlying causal action structure of agents is an important first step to understand the dynamics of a given system, and also to assess what types of structure are really

informative about future states of complex systems. Assuming that the actions of some agents trigger the actions of some other (or same) agents, we propose here a generic method to infer such causal lead-lag activity networks and to exploit their presence with machine learning methods so as to predict the dynamics of macroscopic quantities. Although the method is generic, we focus here on financial markets, because the traders' behavior leads to maximally unpredictable dynamics because all of them try to learn as much as possible to exploit any potential predictability [4]. The fact that dynamics becomes predictable in the most unpredictable complex systems when on accounts for agent lead-lag activity networks demonstrates the potential of our method.

Since a sizable proportion of financial activity is endogenous [12, 19], i.e. triggered by past activity, we shall illustrate how financial markets become predictable if the trader lead-lag activity network is persistent enough. While most of available financial data is fully anonymous, some financial actors such as brokers have access to trader-resolved data: to each order is associated a client identification number. Brokers are interested in managing the risk associated to their temporary inventory against future price moves or large volume imbalance (buy-sell). How much predictability either of order imbalance or of average transaction price change trader-resolved data brings is an open question. Here, we take the point of view that predictability of complex systems such as financial markets is due in part to an underlying structure of systematic lead-lag between the actions of traders. Because of the large quantity and high quality of data generated by brokers, financial markets provide an ideal testing ground for the new method we introduce and to illustrate this point of view.

This work is relevant to several types of market participants who try to match buy and sell order flows (which are submitted asynchronously) by keeping some of them in their inventory. Order crossing may thus occur if incoming orders can be matched against current inventory or added to it and made available for future matching, which may happen at many levels. For example, two strategies of an investor may have opposite opinions about the same asset at about the same time, in which case internal crossing saves transaction fees and reduces uncertainty. If an order needs to be sent to an exchange, it may be matched on its way at crossing networks, dark pools, or even at an internal matching system within the exchange (e.g. IMS at NYSE Euronext) [20].

Managing one's inventory in this situation is of great practical importance, as keeping an inventory is risky. A standard approach would be to solve a stochastic optimization problem and to minimize some cost function (e.g. risk or probability to reach an inventory limit) over a given time horizon, usually with stochastic processes without any predictability both for the order flow and the future prices. Here, we consider this situation as an on-line prediction problem instead and show how being able to identify the source of orders makes it possible to predict the direction of both the order flow and the volume weighted average price (VWAP) for retail clients.

Accordingly, we focus here on matching engines that are able to identify the

source of the order (strategy, investor, broker, etc.). We link order flow and VWAP direction prediction with the existence and persistence of trader lead-lag networks which encode how the activity of some traders (e.g. buy) systematically leads on that of other traders (e.g. sell). Our first contribution is to introduce an unsupervised method to infer such networks which is generic enough to be applied at all levels of order crossing and in non-financial contexts in which the similarity of choices of items by customers may be used to predict future actions. The method consists in first clustering traders into groups according to their synchronicity with the method of [38], determining the aggregate state (buy/sell/neutral) of each group and then applying the same method to lagged group states to detect systematic lead-lag between groups. While synchronicity is likely due to the use of the same strategies or of the same source of information, or both, lead-lag networks are likely caused by the different reaction speed of the respective strategies (e.g. two moving averages with different parameters); an alternative explanation is that some traders react with different delays to common information [6, 24].

If these trader lead-lag networks are sufficiently persistent, some quantities become predictable. First, order flow is predictable if the state of groups (buy/sell/neutral) is partially causal. In addition, proper inventory management requires to predict price directions as well. Our second main contribution is thus to assess the predictability of both order flow and price direction. Only the simplest prediction scenario is studied: we try to predict the sign of each quantity from the global state (buy, sell, neutral) of each trader group and their lagged values. In other words, we reduce prediction to a classification problem from discrete variables and use standard methods of machine learning. This setup is both crude and robust to outliers. The point is not to provide a finely tuned method to manage inventory for brokers, but to provide evidence that the persistence of lead-lag trader networks yields successful predictions.

1.1. *Literature review*

Our contribution is related to several areas of finance pertaining to order flow segmentation, predictability, and inventory control by an informed market maker.

The first broad related area is market making in the presence of predictable order flow. In the context of market microstructure, the role of meta-orders in the long memory of the sign of market orders is well documented [31, 5]. The order flow of individual traders is known to be anti-correlated with previous daily or weekly price returns [17, 25]. A related topic, although less directly relevant to our contribution, is the predictive power of order flow on other quantities than itself such as price returns [26]. Whereas market makers were assumed to be fighting against informed traders in the early literature, the long memory of market order signs leads to a new paradigm of optimal market making [1]. Internal order matching differs from market making at an exchange in that one may liquidate in part one's inventory at the exchange, although with non-negligible transaction costs [15].

4 CHALLET, CHICHEPORTICHE, LALLOUACHE, KASSIBRAKIS

Trader grouping is often performed according to their role in financial markets (e.g. individual investor, institutional investor, etc). Average properties are then computed over whole sub-populations [17, 23, 18, 2].

Unsupervised clustering on the other hand rests on the similarity of actions of traders determined *ex post*. The simplest approach is based on the computation of the correlation matrix of trader inventory changes; then Principal Component Analysis is used together with Random Matrix Theory (to account for the finite length of the available time series) to extract eigenvalues outside the random spectrum [41, 32, 40]. It turns out that at a timescale of a single day, only one or two eigenvalues stand out of the noise spectrum, the largest being associated with previous price returns. This allows one to classify traders as mean-reverting (the majority of them), trend-following, and non-classifiable. The drawback of this approach is that linear correlations do not capture the full correlation structure of traders. In addition it fixes the number of categories of traders.

An alternative approach is Statistically Validated Networks (SVNs) [39] which consists in computing a similarity score between two agents according to how synchronous and similar their activity and inactivity periods are. This method is generic and works well provided that the number of possible states (active, inactive, etc) is small: one determines a p-value of synchronousness and establishes a link between two agents in a statistically sound way. Once all the links between all pairs of agents are tested, one obtains the full synchronousness network of agents. [38] find a surprising degree of synchronization within groups of Finnish traders at a daily timescale.

Lead-lag relationships between traders are much less studied. For lack of available trader-resolved data, the literature has focused on lead-lag relationships between price returns [27, 37, 21, 10]. Lead-lag relationships between traders are discussed in the context of various time scales of contrarian behavior [6, 24]. We are not aware of any work on unsupervised inference of lead-lag between traders.

2. Data description and notations

We work with datasets on foreign exchange (FX) transactions from two independent sources: a large dealing bank (LB hereafter^a), and a broker-dealer (Swissquote Bank SA, SQ hereafter^b). We refer the reader to [20] for more details about the FX market organization. Both datasets contain information about all the trades of their clients over a given period: anonymous client identification number, trade time with a millisecond precision, traded currency pair, signed volume, and price (currency

^aLB's electronic market-marking desk provides liquidity (i.e. quotes and volumes) on the currency rates to large clients such as commercial companies, financial institutions, pension funds, hedge-funds.

^bSQ acts as an on-line broker on thousands of financial instruments, with a large market share in the global Foreign eXchange activity in Switzerland. Its clients range from retail investors to asset managers and institutions.

Dataset	Timespan	Instruments	Traders	Trades
SQ 2012	31 Jan. 2012 → 10 Aug. 2012	68	$> 10^3$	$> 10^6$
SQ 2014-6	01 July 2014 → 15 March 2016	206	$> 10^4$	$> 10^7$
LB	01 Jan 2013 → 17 Sep. 2014	12	$> 10^4$	$> 10^6$

Table 1. Basic statistics of the datasets.

Dataset	Pair	Traders	Trades
SQ 2012	EURUSD	$> 10^3$	$> 5 \times 10^5$
SQ 2014-6	EURUSD	$> 10^4$	$> 10^6$
	EURGBP	$> 5 \times 10^3$	$> 5 \times 10^5$
	USDJPY	$> 10^4$	$> 10^5$
LB	EURUSD	7300	5×10^5

Table 2. Basic statistics of the datasets for the three studied pairs.

rate). A summary of the datasets structure and contents is provided in Table 1.

This paper focuses on the most traded pairs only. Accordingly, Table 2 gives a breakdown of descriptive statistics of the studied pairs. For confidentiality reasons, we cannot give more precise figures for SQ.

2.1. Number of transactions per trader

The number of transactions n per trader per year for a given asset in equity markets has been reported to have heavy tails which may be approximated by a power-law $P(n) \sim n^{-\alpha}$ with tail exponent $\alpha \simeq 2$ [38]. This means that some traders are orders of magnitude more active than others, which implies that focusing on the most active traders may simplify much the prediction of future order flows. We checked that the power-law still holds on FX markets over about 2 decades of n ; the exponent α was estimated for each currency and each year with the method introduced by [9] (see also [16]). For a given currency pair, we filtered out the years in which less than 1000 traders were active, which left 53 estimates. We found $\alpha_{avg} \simeq 1.99 \pm 0.07$ (95% confidence interval) in the largest dataset (SQ 2014-6).

2.2. Trade size

The different nature of the respective clients of LB and SQ influences the typical trade size. We present the results in multiple of 1000 of the base currency for SQ clients and in multiple of 100'000 for LB clients. In Fig. 1, we plot the distribution

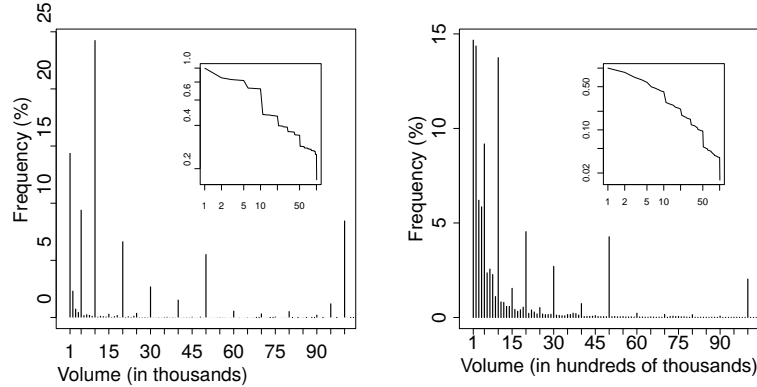


Fig. 1. Distribution of EURUSD trade sizes. Left: SQ. Right: LB. Inset: cumulative tail distribution, in log-log scale.

of the transaction sizes for the EURUSD. Similar results are obtained for other pairs. We observe peaks at round size (10,20,50,...), with a stronger effect for SQ than for LB, which is consistent with the fact that its clients are mostly individual traders, therefore more prone to be affected by psychological biases than institutional traders (see a discussion about this phenomenon in the FX EBS market in [28]).

3. Inference of lead-lag networks

Although lead-lag networks can be determined between the agents themselves, clustering the traders simplifies the visualization of lead-lag networks and is very useful (and a standard procedure) before calibrating machine learning methods which often are confused if two or more predictors are very correlated. This is the case here: because many FX traders are algorithmic traders, their activity/inactivity is very similar when they use the same algorithms. Thus, grouping traders encodes the systematic use of the same set of strategies (which includes news sources) and does not reduce the predictive ability of our method.

3.1. Clustering traders by their synchronicity

Since the lead-lag method we propose is an extension of the SVNs, it is worthwhile explaining the method in some details.

3.1.1. Method

Statistically Validated Networks (SVN) were introduced in [39] and applied to the clustering of Finnish investors in [38]. The technique aims at characterizing the degree of synchronization between the actions of two traders, thus, by extension,

at identifying groups of traders who act in a similar way. By definition, it is an unsupervised clustering method.

The first step is to cut time into slices of equal length δt ; we chose arbitrarily $\delta t = 1$ hour. In practice, the duration of each slice must be adapted to each situation. In the case of the FX traders in our dataset, 1 hour is a reasonable choice with respect to typical trading patterns of active traders. We define time slice t as the interval $[t, t + \delta t]$. For each time slice t , we classify the state of all traders into buying (state +1), selling (state -1), neutral (state 2), and inactive (0). Denoting the total signed volume of trader i during time slice t by $V_i(t)$ and the sum of the absolute trading volume of the transactions of trader i during time slice t by $G_i(t)$, one defines the imbalance ratio $\rho_i(t) = V_i(t)/G_i(t)$. The imbalance ratio characterizes the trader as a net buyer ($\sigma_i(t) = 1$) if $\rho_i(t) > \rho_0$ (ρ_0 being a small threshold), as a net seller ($\sigma_i(t) = -1$) if $\rho_i(t) < -\rho_0$, as neutral ($\sigma_i(t) = 2$) if $|\rho_i(t)| < \rho_0$, or as inactive ($\sigma_i(t) = 0$) if $V_i(t) = G_i(t) = 0$. The choice of $\rho_0 \in [0.01, 0.1]$ is not crucial; in the following we set $\rho_0 = 0.01$. Because the following analysis focuses on the most active traders, the inactive state will be dropped.

The synchronicity of a pair of traders is measured by counting the co-occurrences in the time series of their states, and attributing a p-value that reflects the statistical significance of this synchronicity assuming pure randomness. To deal with the testing of all pairs of traders for each of the 9 types of co-occurrences of states $\{-1, 2, 1\} \times \{-1, 2, 1\}$, a multiple hypothesis testing correction is needed. We choose to use the False Discovery Rate [3] with a rate set to $p_0 = 0.05$. A network is built by validating links between pairs of traders if the p-value of their synchronization is smaller than the FDR-corrected threshold; traders without any links are dropped (see [38] for more details). Note that contrarily to one-shot statistical testing, for which such value of p_0 would be foolishly large and which does not control the false discovery rate (i.e. false positives), we are dealing here with a population of p-values in which the FDR is controlled. In other words, there is on average a p_0 fraction of false links in the SVNs that we determine. Since we are mostly interested in groups, this value is not crucial.

The resulting network consists most of the time in a large connected component (i.e. a large group of connected traders) and other very small disconnected components. The large connected component is further decomposed into communities (or modules). Many methods have been designed to detect communities in complex networks (see e.g. [30] for a review). As in [38], we use the InfoMap method [35], which segments a connected network according to a maximum entropy argument. While this method is not suited for multi-links networks, it can deal with weighted networks. Therefore an easy workaround consists in converting multi-links into weighted links by assigning a weight equal to the number of validated links between two traders. When applying community detection, we exclude links between opposite action (buy-sell), as we are primarily interested in finding groups of traders that act in the same direction at the same time so as to be able to aggregate the volume of a given group and compute a meaningful measure of its state.

8 CHALLET, CHICHEPORTICHE, LALLOUACHE, KASSIBRAKIS

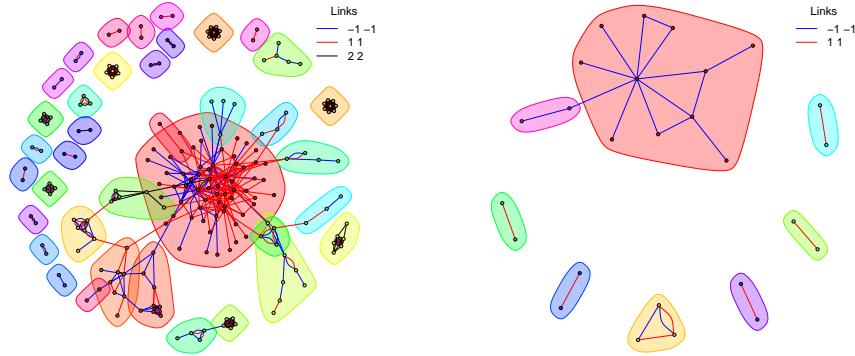


Fig. 2. Projection of typical networks of traders, determined at the hourly time scale (EURUSD). Every link between two traders is statistically validated and labelled by the equal-time behavior of the pair: (1,1) if both are net buyers, (-1,-1) if both are net sellers, (2,2) if both are neutral. The InfoMap community detection method additionally provides clusters, shown in colors. Left: SQ 2012. Right: LB.. These are bi-dimensional projections of complex networks in which horizontal and vertical directions have no special meaning.

3.1.2. Trader synchronicity network descriptive statistics

In the following, for each in-sample time window, we keep the 500 most active traders and filter out those with less than 100 trades. We exclude weekends as trading activity then is markedly different (and much smaller) than that of business days. In addition, some traders do not use algorithmic trading, which restricts their activity periods, or prefer to trade during the most active hours. This is why we only keep trades from 9am to 4pm (London time).

Hourly time slices also allow the building of SVNs over a few months, which opens the way to a large-scale investigation both of the time evolution of SVNs and of prediction (see Sec. 4). Figure 2 shows representative examples of SVNs computed with hourly time slices over a given time period. The number of clusters is of particular interest: while the number of groups of SQ traders stays roughly constant (and large), a peculiar phenomenon occurs in the four months preceding Jan. 2014 in the LB dataset: Fig. 3 reports that the number of detected groups reaches 1 then, with a similar decrease of the number of links between traders. This implies that our method detected much less statistically validated synchronization during this period. We were not able to find a simple explanation for this phenomenon, but it is clear that the presence of a single group prevents significant lead-lag. We thus expect predictability to be minimal around January 2014 for LB data (which is confirmed in section 4.1.1).

Statistically validated lead-lag networks and inventory prediction in the foreign exchange market 9

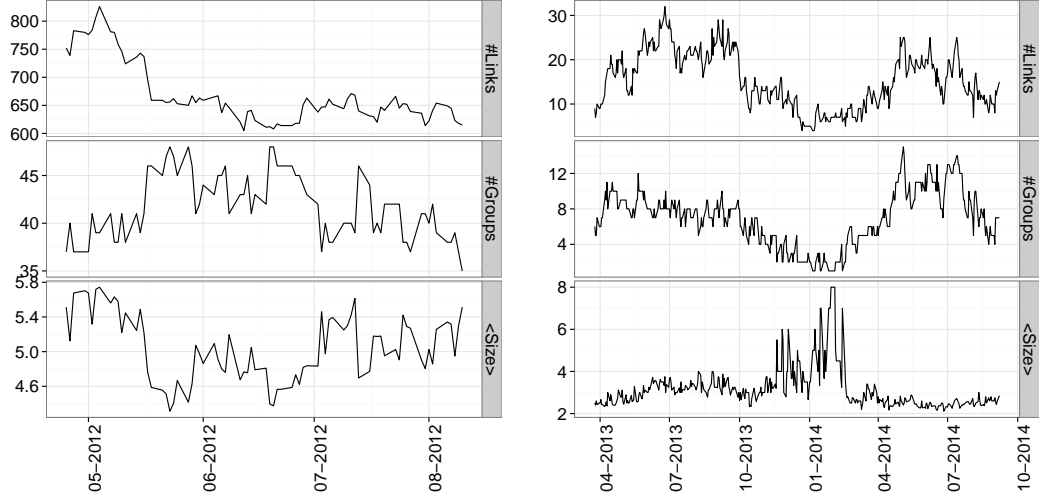


Fig. 3. Network of traders: basic statistics over time (EURUSD). Left: SQ 2012. Right: LB.

3.1.3. Stability of clustering as a function of time

Sliding windows allow us to detect time-varying clustering, which reflects changes of strategy use by the traders as time goes on (as detect by a fixed 1-hour time slices). They also raise the question of the stability of clustering, a necessary condition for the persistence of lead-lag networks, thus for the possibility of predicting order flows.

Assessing clustering stability is made easier by having consistent group labeling. The first step is to make sure that the clustering tools guarantees the constant labeling of groups when the grouping of traders is exactly the same one between two time slices. In practice, a non-negligible proportion of traders does not belong to the same group in the clustering performed at two consecutive times. Thus, the first problem to solve is how to attribute coherent names to clusters as time goes on. The simplest solution is to use a similarity measure between of the grouping at time slices t and $t - 1$ and to propagate the name of cluster g_{t-1} to the most similar cluster at time t . The similarity measure is based on the overlap of the elements of two clusters and defined as

$$OA(g_{t-1}, g'_t) = |g_{t-1} \cap g'_t|, \quad (1)$$

where g and g' are trader groups/clusters and where $|x|$ stands for the number of elements of x . We shall use the normalized overlap measure

10 CHALLET, CHICHEPORTICHE, LALLOUACHE, KASSIBRAKIS

mean(std dev)	LB EURUSD	SQ EURUSD	SQ EURGBP	SQ USDJPY
mean	0.87	0.83	0.91	0.84
standard deviation	0.14	0.09	0.09	0.10
fraction of perfect stability	0.34	0	0.01	0

Table 3. Summary statistics of the Adjusted Rand Index for some currency pairs of both data sources. SQ means SQ2014-6.

$$OP(g_{t-1}, g'_t) = \frac{OA(g_{t-1}, g'_t)}{|g_{t-1} \cup g'_t|} \quad (2)$$

to account for the size of both clusters.

Consistent naming allows us to produce meaningful visualizations. Figure 4 shows how the traders switch between clusters as a function of time, using a so-called “river chart”: at a given time, the traders belonging to the same group are stacked together and form a continuous vertical dash, each group being clearly separated from each other. One then adds the trajectory of each trader from its group at time t and its group at time $t + 1$. Having a consistent group labeling method ensures that if there is strictly no change of group between two time steps, only horizontal stripes appear. Thus, river charts allow us to visualize at the same time group sizes and the evolution of group compositions, i.e. distributional and dynamical properties. There clearly is a large cluster whose size is relatively stable as a function of time. The smallest clusters are much less stable: they merge and split again as time goes on. It is noteworthy that clustering was performed every week in this figure: the cluster structure is relatively stable even at this sampling frequency.

3.1.4. Cluster membership stability

We use the Adjusted Rand Index (ARI thereafter), a standard global measure of clustering stability between two consecutive clustering times [34, 13]. An ARI of 1 denotes perfect clustering stability, while the expected value of ARI for random clustering is 0. The stability of LB traders is perfect (ARI=1) in about a third of the days, which underscores a remarkable level of regularity of LB clients, also hinted at by the large average ARI. Retail clients of SQ are more fickle (possibly because a larger fraction of them do not use algorithmic trading), but their average ARI is also remarkably high (see Table 3). In short, the ARI suggests a strong and encouraging level of clustering stability in all data sets.

3.2. Statistically validated lead-lag networks

Determining validated lead-lag relationships between two time-series essentially consists in detecting synchronicity between the first time series and the suitably lagged

second time series. In other words, one may apply the SVN machinery to the state of agent i and the lagged state of agent j (including the case $i = j$). In the context of investors, since some agents use the same systematic strategies either to open or close a position, or both, and thus act in a remarkably synchronous way, it makes sense to focus on the lead-lag relationships between the groups of traders determined with SVNs and a community detection method.

Once the groups of traders are determined via the SVN method, the procedure works as follows:

- (1) volume imbalances are aggregated at the group level: $V_g(t) = \sum_{i \in g} V_i(t)$ and the state of group g , denoted by $\sigma_g(t)$, is determined in the same way as in the SVN method;
- (2) for each pair of group (g, g') ($g = g'$ is allowed), the p-value of the coincidence between $\sigma_g(t)$ and $\sigma_{g'}(t+1)$ is computed as in the SVN method;
- (3) the number of pairs of groups is N_{groups}^2 because we allow self-linking. Since the number pairs of states is 3×3 , the significance level needs to account for $N_{tests} = 9 \times N_{groups}^2$ tests, thus FDR is used once more. Notice in particular that $g \rightarrow g$ links are not trivial and correspond to auto-correlated time series of aggregated volume imbalance: these links appear as loops in the directed network representation.

Grouping agents has the advantage of simplifying the description of the system state, thus to reduce the dimensionality of the prediction problem. In some cases, it may be useful to skip the grouping step and determine lead-lag between agents.

3.2.1. Results

The same parameters as in Fig. 2 are used for link detection between groups. We display two representative networks in Fig. 5. The most common type of link is to oneself. More complex lead-lag relationships also exist: take group 22 in SQ data set; it typically buys EURUSD within one hour after having sold EURUSD; group 31 does the opposite. One notes that, interestingly, group 31 sells during the hour after group 22 has sold. This means that both groups act in an opposite way provided that group 22 has sold EURUSD in the previous time slice. What is remarkable is this happens in a systematic way.

There are more lead-lag links between SQ groups than between LB groups, especially self-links. Interestingly, more links that validate opposite directions are present in the lead-lag case compared to the contemporaneous one. The evolution of the number of links over time is shown in Fig. 6: sudden drops of the number of lead-lag links are noticeable for all data sets of SQ. Quite logically, there is no lead-lag relationships around January 2014 for the LB dataset, which is to be related to the detection of only one group (see Fig. 3).

The presence of links, valid under severe statistical inspection, clearly demon-

strate the existence of predictability in the investors trading directions. However, predicting trading flows not only requires equal-time clustering stability, but also lead-lag stability. Measuring the latter at the level of traders is more informative than only using lead-lag between groups. Indeed, imagine that at time t , group 1 includes Alice and Bob, and leads on group 2 which contains Carol and Dave. It may happen that at time $t + 1$ group 1 splits into groups 1a and 1b, that the composition of group 2 is conserved, and that groups 1a and 1b still lead on group 2. The point here is that the lead-lag between group 1 and 2 defines *a fortiori* lead-lag relationships between all the traders of group 1 and those of group 2 at time t . The subsequent splitting of group 1 into 1a and 1b does not change the lead-lag relationships between traders. Thus, a suitable lead-lag stability measure is the fraction of lead-lag links between traders that is conserved between two successive clustering times, restricted to the traders that exist at both times. Mathematically, let $\Lambda_{ij}(t \rightarrow t + 1)$ denote the adjacency matrix element of the lead-lag network at the trader level between time t and time $t + 1$, i.e., $\Lambda_{ij}(t \rightarrow t + 1) = 1$ if trader i leads on trader j and 0 otherwise, then the stability measure is defined as

$$\beta(t \rightarrow t + 1) = \frac{\sum_{ij} \Lambda_{ij}(t \rightarrow t + 1) \Lambda_{ij}(t + 1 \rightarrow t + 2)}{\sum_{i'j'} \Lambda_{i'j'}(t \rightarrow t + 1)}$$

Figure 7 reports the time evolution of β . It does fluctuate much, but never quite reaches 0 for long periods, except for LB in January 2014, which, on the whole, leaves hope of successful predictions. However, one readily notices that the number of both validated lead-lag network nodes and links is much smaller for LB data. Whether a high value of β is related to a larger predictive power is investigated in Sec. 4.1.2.

4. The predictability of inventory

We have so far shown the existence of a lead-lag structure whose persistence implies that some quantities are predictable. This does not however mean that e.g. order flows are simple autoregressive models. When one fits ARIMA models and hours of the day as fixed factors, the AIC criterion always suggests to use a ARIMA(0,0,0) model: at this time scale, the only relevant factors are the hours of the day.

These networks also give crucial insights about how to make predictions from trader-resolved data. While future actions do depend on the current state of all groups, any prediction method must also be fed with the lagged group states, so that the lead-lag networks can be learned and exploited as well.

4.1. Order flow

For the sake of simplicity, we have restricted the group states to their discrete values $\{-1, 2, +1\}$. This strongly suggests to predict the sign of the total order flow, instead of its exact value. More precisely, we aim to predict $v(t + 1) = \text{sign}(\sum_i V_i(t + 1))$,

where i sweeps over all the traders from a set P of predictors consisting in the states of the groups, denoted by $\sigma_{g,t}$ (determined in-sample by SVNs), their lagged values $\sigma_{g,t-1}$ and the time of the day. Including lagged group states is consistent with the existence of group lead-lag of order one and is therefore necessary. This amounts to classify $v(t+1)$ into $\{-1, 0, +1\}$, from the knowledge of group states up to time t .

The training phase is summarized by $P_{t_0,t_1} \sim W_{t_0+1,t_1+1}$, where P_{t_0,t_1} is a matrix of predictors and W_{t_0+1,t_1+1} the vector of the quantity to be predicted; more precisely,

$$P_{t_0,t_1} = \begin{pmatrix} \sigma_{1,t_0} & \sigma_{2,t_0} & \sigma_{1,t_0-1} & \sigma_{2,t_0-1} & h(t_0) \\ \vdots & \vdots & \vdots & \vdots & \vdots \\ \sigma_{1,t_1} & \sigma_{2,t_1} & \sigma_{1,t_1-1} & \sigma_{2,t_1-1} & h(t_1) \end{pmatrix} \sim \begin{pmatrix} v_{t_0+1} \\ \vdots \\ v_{t_1+1} \end{pmatrix} = W_{t_0+1,t_1+1}, \quad (3)$$

where the symbol \sim implies that there is some kind of (possibly highly non-linear) relationship between a line of P_{t_0,t_1} and the corresponding next global trading flow imbalance, as suggested by the validated lead-lag networks plotted in Fig. 5. Because P_{t_0,t_1} also contains the time of the day, subtle hourly differences of these validated lead-lag networks may be detected as well. Note that we do not feed the lead-lag networks to the machine learning method, but the latter exploits them in an implicit way. In addition, P_{t_0,t_1} may also include group states lagged more than once. Many variations of Eq. (3) are relevant. First, instead of the group states, one can input the actual volume (or log-volume), v may also be the VWAP or future price returns (see section 4.2), etc. At all rates, we focus on the simplest possible setting here.

The discrete nature of v_t suggests to infer the \sim relationship with logistic regression, which does not lead to satisfactory results (see appendix A where they are reported). Off-the shelf machine learning methods outperform logistic regression thanks to their more non-linear nature; we thus will focus on such methods. Instead of trying and comparing many machine learning methods and tuning their parameters until seemingly finding predictability, we chose a single method known for its robustness and performance: plain random forests (RF) [7, 22], which have many useful features in this context: first, they avoid in-sample over-fitting, they are robust, non-linear and possess an overall very good predictive power without tweaking any parameter (at least on many “standard” data-sets [11]). A bonus is the availability of the relative importance of each predictor. As a consequence, we will be able to check that group states, i.e., lead-lag, is on average more important than the time of the day. For the sake of computation speed, calibration was performed every day, not every hour. Thus, predictions for a given day rest on a calibration that uses data up to the previous day.

We chose 10 calibrations window lengths, denoted by T_{in} , ranging from 45 to 90 week days (9 to 18 weeks) with common difference of 5 days (1 week). Although RFs output classification probabilities, i.e., the probability that the sign of the next order flow will be $+1$, say, we take the most probable predicted state as the prediction of a

given RF. In addition to computing the respective performance of each calibration length, we also performed a majority vote of the predictions originating from each timescale. If +1 and -1 obtain the same number of votes, the prediction is set to zero. Finally, we used the package RandomForestSRC [22] and did not tune any parameter of the RF calibration function.

4.1.1. Results

We run the procedure on the three most traded pairs of the SQ 2014-6 dataset and on EURUSD LB dataset. Figures 8 to 9 report the out-of-sample performance of our method. Although we train RFs on the signs of order flow, we also plot the cumulated performance in currency units. In essence, if the prediction of the order flow signs is successful during the most active periods, it also predicts the actual order flow itself, on average. This the case of SQ clients, but not for LB: the most precise sign predictions are during lunch time, i.e. when the activity reaches a local minimum.

A possible explanation for this is the clear difference between SQ and LB clients: whereas the cumulated net imbalance of SQ clients is mostly mean-reverting, that of LB clients keeps on increasing. This means that SQ clients are mostly speculators, while LB clients use the FX market for other purposes than mere speculation, on average.

Let us now apply statistical tests to the out-of-sample performance in currency units: for both brokers and all pairs, the out-of-sample performance is clearly significant. However, the real question is the predictive power of our methodology regarding the sign of the next order flow. Chou and Chu approach consists in testing whether A predicts B , where A and B are binomial variables, taking into account auto-correlations, the null hypothesis being that A does not predict B [8]. When applied to SQ data, this test unambiguously shows that our method yields predictive answers, and that it is not useful in the case of LB data. This may mean that an hourly time scale may not be a wise choice for LB traders.

A different way to look at these results is to analyse the performance conditioned on the hour of the day. In Fig. 11, we report the p-values of out-of-sample performance conditional on the hour of the day. We notice a tendency to perform well in periods of high activity for SQ clients, not for LB clients.

Adding the returns to the feature set did not improve the forecast, probably

because the returns effect are already embedded in groups actions, in line with the factor analysis of [32]. Remarkably, multiple runs of the procedure revealed that there is no need to update the model every day: an update every 5 days approximately gave the same results, which is consistent with the large persistence, on average, of lead-lag networks.

4.1.2. Importance of predictors

In order to check that the order flow imbalance depends on the group states we check *a contrario* that the hour of the day is not the most important predictor most of the time. That the non-linear relationship between the predictors and future order imbalance signs sometimes depends on the hour of the day is not surprising, as indeed some groups may be more active at certain times of the day. However, given the existence of lead-lag networks, we do not expect the hour of the day to top the list of variable importance very often.

There are several ways to measure variable importance in Random Forests; we have used the standard Breiman-Cutler measure, which (roughly speaking) consists in shuffling the elements of a given column of the predictors matrix and determining how the in-sample prediction error changes (see [7] for more details). We shall focus on the rank of the hour of the day relative to the one of all the other columns. Since we use an unsupervised method to cluster the traders, the number of groups varies as a function of time. As a consequence, we define the rank ratio of column h as the ratio between the rank of the importance of h , denoted by $\text{rank}(h)$, 1 being the most important, and the number of columns of P , denoted by K_{t_1} . Because a rank of 1 would correspond to $1/K_{t_1}$, a time varying quantity, and might therefore make it unnecessarily difficult to compare two rank ratios, we define the adjusted rank ratio of h as

$$r_h = \frac{\text{rank}(h) - 1}{K_{t_1} - 1}.$$

With this convention, the hour column is the most important predictor if $r_h = 0$ and the least important one if $r_h = 1$. The left plot of Fig 12 plots r_h as a function of time for EURGBP. It turns out that the distribution of the relative importance of h is rather bimodal (see the histogram in the middle plot of the same figure) and persistent. The bimodal nature of r_h is less pronounced for other T_{in} and currency pairs. At all rates, one may wonder if prediction is more successful in periods of low r_h or high r_h , or equivalent, how predictive of success r_h is. As we deal with a classification problem, the tool of choice is Receiver Operating Characteristic (ROC) curves and their associated Area Under Curve (AUC), which, in a nutshell, quantifies how different the distribution of r_h is when the prediction is correct and when it fails. By definition, an AUC of 0.5 corresponds to the absence of predictive power of r_h , while an AUC of 1 implies that r_h fully determines the success of predictions. The right plot of the same figure makes it clear that there is some

predictability associated to r_h , and that it is once again larger during the most active hours. Since there is only one value of r_h for each day, and since one makes one prediction per hour, we have computed average AUC conditional on the hour of the day.

Finally, we compute the hourly average AUC of the trader-trader lead-lag persistence β . Figure 13 reports the AUC for the three SQ currency pairs as a function of the number of weeks of the calibration window, restricted to the same out-of-sample period. Once again, the predictive power of such measure is weak.

4.2. VWAP prediction

Managing one's imbalance requires more than predicting the sign of the order flow. Indeed, succeeding in predicting the average direction of the trades during the next period is also necessary. Instead of predicting separately the sign of the next price return, we focus on the VWAP of the trades of the broker's clients during each time slice as it combines both volume and price. If a broker can predict the evolution of his VWAP in the next time slice, then it will be able to manage much more efficiently its inventory.

The setup is very similar as that for order flow prediction, except that the vector v_{t+1} to predict now contains the signs of the changes of the broker's VWAP. In other words, we still face a classification problem, but for the VWAP signed difference this time. We keep the same parameters as before. Figure 14 displays the results for EURUSD and SQ: predictability is clearly significant and even better than for the sign of the order flow. Figure 15 shows that the predictability of the sign of VWAP change is particularly significant at the most active hours for all currency pairs for SQ. LB customers on the hand show once again exactly the opposite behavior: prediction ability is the worst during the most active hours: VWAP change is not predictable if the order flow signs are not.

5. Conclusion and perspectives

Our aim was first to introduce an unsupervised lead-lag network inference method and show the existence of persistent agent lead-lag networks in financial data. Quite remarkably, these hidden causal networks open the way to useful predictions at a one-hour time horizon in one of the most unpredictable complex systems. Admittedly, we used more detailed (and private) information than most market participants can obtain: the point is that this kind of information makes the origin of predictability explicit. Reversely, one then understands why predictability is not significant when lead-lag networks are too sparse, either because the trader activity

similarity is too small or because the chosen timescale does not correspond to the natural activity rate of the agents.

Being able to predict the evolution of one's inventory is very useful in practice for improving internal order matching and inventory management, in particular with respect to risk constraints. This implies that theoretical results about inventory management must be generalized in order to include predictability both of order flow and VWAP (e.g. [15]).

Avoiding overfitting was one of the focus of the applied part of this paper. However, substantial improvements to the learning methods can easily be achieved. First, more relevant information can be added to predictors, such as the group states lagged more than once. This will be helpful if some traders have typical holding periods larger than the duration of time slices. In addition, we have not exploited the full potential of random forests, which do not output binary predictions, but the fraction of trees that predict a given state. Finally, simple learning schemes such as follow-the-leader may improve much the aggregation of the predictions from each time-window calibration lengths, hence the overall prediction performance. These kind of methods simple are likely to exploit better the available information without adding sources of overfitting.

We have also avoided method overfitting by using a single machine learning method without trying to vary any of its parameters. Improvements to random forests such as oblique Random Forests [33], or boosted trees [14], may yield better performance. This would also open the way to ensemble learning. Finally, while we arbitrarily chose one-hour time slices, one should investigate lead-lag networks at various time scales at the same time.

On a more philosophical note, our work is a first step towards the understanding of what triggers the activity of an investor, one of the current mysteries in Finance. We cannot explain yet why a group of traders acts at time t . However, their activity depends on the past activity of some other groups or themselves, which is expected since most trading activity is self-referential in financial markets. The fact that VWAP changes are predictable points out that traders react at least in part to past the direction of past price changes. This recursive (thus indirect) answer to a fundamental question also deserves further investigation, in particular with a multiple timescales approach.

Finally, coming back to complex systems, this work shows how an unpredictable complex system becomes predictable once agent-resolved data is simplified and prepared so as to make lead-lag networks learnable, which promises to improve ones' tools to manage risk dynamically. Future work will estimate how predictable agent behavior is in other contexts such as communication networks and on-line shopping.

References

- [1] Avellaneda, M. and Stoikov, S., High-frequency trading in a limit order book, *Quantitative Finance* **8** (2008) 217–224.

18 CHALLET, CHICHEPORTICHE, LALLOUACHE, KASSIBRAKIS

- [2] Barber, B., Lee, Y., Liu, Y., and Odean, T., Just how much do individual investors lose by trading?, *Review of Financial Studies* **22** (2009) 609–632.
- [3] Benjamini, Y. and Hochberg, Y., Controlling the False Discovery Rate: A Practical and Powerful Approach to Multiple Testing, *Journal of the Royal Statistical Society. Series B (Methodological)* **57** (1995) 289–300.
- [4] Bouchaud, J.-P. and Challet, D., Why have asset price properties changed so little in 200 years, in *Econophysics and Sociophysics: Recent Progress and Future Directions* (Springer, 2017), pp. 3–17.
- [5] Bouchaud, J.-P., Farmer, J. D., and Lillo, F., How markets slowly digest changes in supply and demand, in *Handbook of Financial Markets: Dynamics and Evolution*, eds. Hens, T. and Schenk-Hoppè, K. (Elsevier, 2009), pp. 57–160.
- [6] Boudoukh, J., Richardson, M. P., and Whitelaw, R., A tale of three schools: Insights on autocorrelations of short-horizon stock returns, *Review of financial studies* **7** (1994) 539–573.
- [7] Breiman, L., Random Forests, *Machine Learning* **45** (2001) 5–32.
- [8] Chou, C. and Chu, C.-S. J., Testing independence of two autocorrelated binary time series, *Statistics & probability letters* **80** (2010) 69–75.
- [9] Clauset, A., Shalizi, C. R., and Newman, M. E., Power-law distributions in empirical data, *SIAM review* **51** (2009) 661–703.
- [10] Curme, C., Tumminello, M., Mantegna, R. N., Stanley, H. E., and Kenett, D. Y., Emergence of statistically validated financial intraday lead-lag relationships, *Quantitative Finance* (2015) 1–12.
- [11] Fernández-Delgado, M., Cernadas, E., Barro, S., and Amorim, D., Do we Need Hundreds of Classifiers to Solve Real World Classification Problems?, *Journal of Machine Learning Research* **15** (2014) 3133–3181.
- [12] Filimonov, V. and Sornette, D., Quantifying reflexivity in financial markets: Toward a prediction of flash crashes, *Physical Review E* **85** (2012) 056108.
- [13] Fraley, C., Raftery, A. E., Murphy, T. B., and Scrucca, L., mclust version 4 for R: Normal mixture modeling for model-based clustering, classification, and density estimation (2012).
- [14] Friedman, J., Hastie, T., Tibshirani, R., *et al.*, Additive logistic regression: a statistical view of boosting (with discussion and a rejoinder by the authors), *The annals of statistics* **28** (2000) 337–407.
- [15] Gallien, F., Kassibrakis, S., Malamud, S., and Passerini, F., Managing inventory with proportional transaction costs, *Available at SSRN 2788593* (2016).
- [16] Gillespie, C. S., Fitting heavy tailed distributions: The powerLaw package, *Journal of Statistical Software* **64** (2015) 1–16.
- [17] Grinblatt, M. and Keloharju, M., The investment behavior and performance of various investor types: a study of Finland’s unique data set, *Journal of Financial Economics* **55** (2000) 43–67.
- [18] Grinblatt, M. and Keloharju, M., Sensation Seeking, Overconfidence, and Trading Activity, *The Journal of Finance* **64** (2009) 549–578.
- [19] Hardiman, S. J., Bercot, N., and Bouchaud, J.-P., Critical reflexivity in financial markets: a Hawkes process analysis, *The European Physical Journal B* **86** (2013) 442.
- [20] Harris, L., *Trading and exchanges: Market microstructure for practitioners* (Oxford University Press, 2002).
- [21] Huth, N. and Abergel, F., High frequency lead/lag relationships—empirical facts, *Journal of Empirical Finance* **26** (2014) 41–58.
- [22] Ishwaran, H. and Kogalur, U., *Random Forests for Survival, Regression and Classification (RF-SRC)* (2016), <https://cran.r-project.org/package=randomForestSRC>,

r package version 2.4.1.

- [23] Jackson, A., The aggregate behaviour of individual investors (2004).
- [24] Jegadeesh, N. and Titman, S., Overreaction, delayed reaction, and contrarian profits, *Review of Financial Studies* **8** (1995) 973–993.
- [25] Kaniel, R., Saar, G., and Titman, S., Individual investor trading and stock returns, *The Journal of Finance* **63** (2008) 273–310.
- [26] Kelley, E. K. and Tetlock, P. C., How wise are crowds? insights from retail orders and stock returns, *The Journal of Finance* **68** (2013) 1229–1265.
- [27] Kullmann, L., Kertész, J., and Kaski, K., Time-dependent cross-correlations between different stock returns: A directed network of influence, *Physical Review E* **66** (2002) 026125.
- [28] Lallouache, M. and Abergel, F., Tick size reduction and price clustering in a FX order book, *Physica A: Statistical Mechanics and its Applications* **416** (2014) 488–498.
- [29] Lamper, D., Howison, S. D., and Johnson, N. F., Predictability of large future changes in a competitive evolving population, *Physical Review Letters* **88** (2001) 017902.
- [30] Lancichinetti, A. and Fortunato, S., Community detection algorithms: A comparative analysis, *Phys. Rev. E* **80** (2009) 56117.
- [31] Lillo, F. and Farmer, J. D., The long memory of efficient markets, *Non-lin. Dyn. and Econometric* **8** (2004).
- [32] Lillo, F., Moro, E., Vaglica, G., and Mantegna, R. N., Specialization and herding behavior of trading firms in a financial market, *New Journal of Physics* **10** (2008) 43019.
- [33] Menze, B., Kelm, B., Splithoff, D., Koethe, U., and Hamprecht, F., On Oblique Random Forests, in *Machine Learning and Knowledge Discovery in Databases SE - 29*, eds. Gunopulos, D., Hofmann, T., Malerba, D., and Vazirgiannis, M., *Lecture Notes in Computer Science*, Vol. 6912 (Springer Berlin Heidelberg, 2011), ISBN 978-3-642-23782-9, pp. 453–469.
- [34] Rand, W. M., Objective criteria for the evaluation of clustering methods, *Journal of the American Statistical association* **66** (1971) 846–850.
- [35] Rosvall, M. and Bergstrom, C. T., Maps of random walks on complex networks reveal community structure., *Proceedings of the National Academy of Sciences of the United States of America* **105** (2008) 1118–23.
- [36] San Miguel, M., Johnson, J. H., Kertesz, J., Kaski, K., Díaz-Guilera, A., MacKay, R. S., Loreto, V., Erdi, P., and Helbing, D., Challenges in complex systems science, *The European Physical Journal Special Topics* **214** (2012) 245–271.
- [37] Tóth, B. and Kertész, J., Increasing market efficiency: Evolution of cross-correlations of stock returns, *Physica A: Statistical Mechanics and its Applications* **360** (2006) 505–515.
- [38] Tumminello, M., Lillo, F., Piilo, J., and Mantegna, R. N., Identification of clusters of investors from their real trading activity in a financial market, *New Journal of Physics* **14** (2012).
- [39] Tumminello, M., Miccichè, S., Lillo, F., Piilo, J., and Mantegna, R. N., Statistically Validated Networks in Bipartite Complex Systems, *PLoS ONE* **6** (2011) e17994.
- [40] Zhou, W.-X., Mu, G.-H., and Kertesz, J., Random matrix approach to the dynamics of stock inventory variations, *New Journal of Physics* **14** (2012) 93025.
- [41] Zovko, I. and Farmer, J. D., Correlations and clustering in the trading of members of the London Stock Exchange, in *AIP Conference Proceedings*, Vol. 965 (AIP, 2007), ISSN 0094243X, pp. 287–299, doi:10.1063/1.2828747, <http://scitation.aip.org/content/aip/proceeding/aipcp/10.1063/1.2828747>.

20 *CHALLET, CHICHEPORTICHE, LALLOUACHE, KASSIBRAKIS*

EURCHF	RF	logistic	EURGBP	RF	logistic	USDJPY	RF	logistic
Chou Chu	3.5e-06	4.8e-05	Chou Chu	8.2e-05	3.6e-04	Chou Chu	4.8e-05	7.9e-01
t	5.0e-12	2.4e-05	t	4.7e-03	1.8e-04	t	4.7e-03	3.9e-01
Wilcoxon	3.9e-13	1.3e-05	Wilcoxon	5.0e-05	4.2e-05	Wilcoxon	4.0e-06	1.7e-03

Table 4. P-values of various tests for positive performance for logistic regression and random forests (RF) on SQ2014-6 dataset.

Appendix A. Prediction with logistic regression

For the sake of meaningful comparisons, we gave to logistic regression the same inputs as to random forests (but split the hour of the day into separate factors), used the same calibration window lengths, and fitted a logistic model every day. The prediction of the model is then rounded to either -1 or +1. The performance summary statistics corresponding to the majority vote between all the calibration window lengths both for logistic regression and random forests are reported in Table 4. It is quite clear that logistic regression is out-performed by random forests.

Statistically validated lead-lag networks and inventory prediction in the foreign exchange market 21

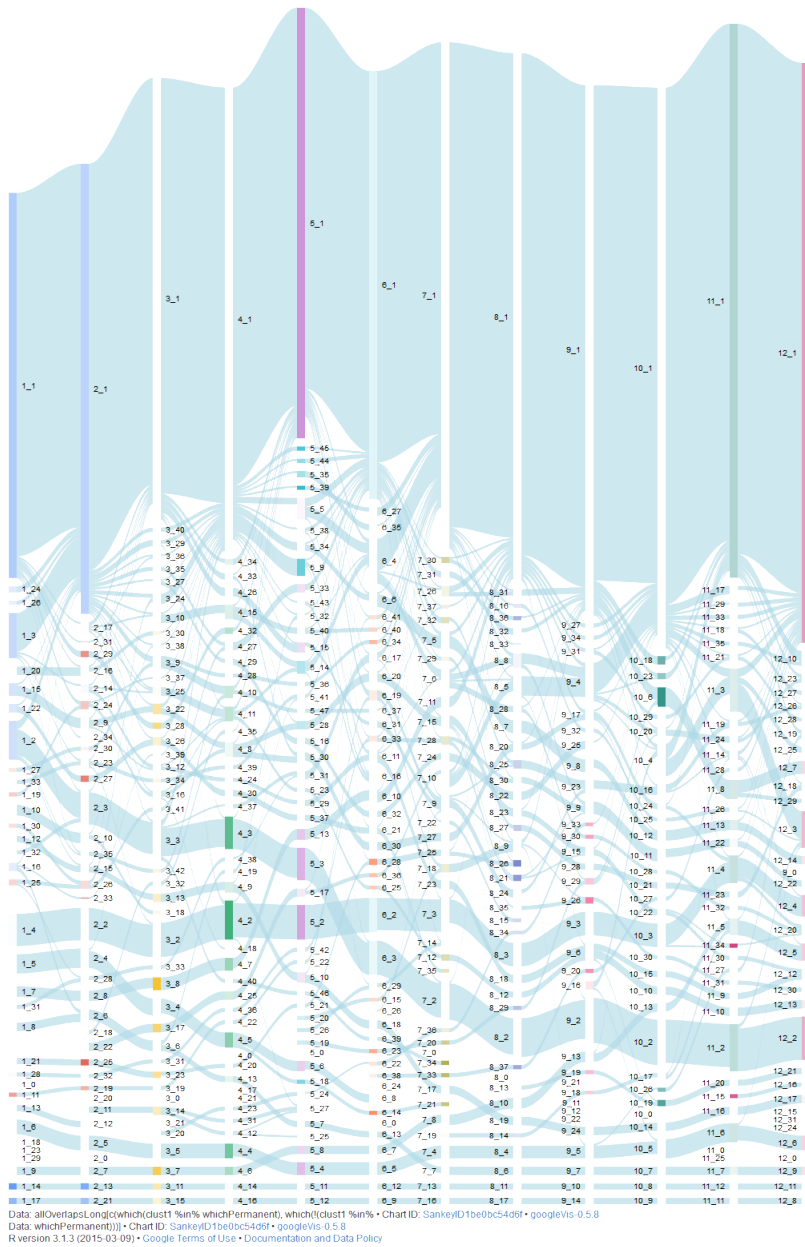


Fig. 4. Agent clustering time evolution. Each elementary line width represents the trajectory of an agent from one group to another group. Hourly time slices, 12 weeks in-sample, weekly clustering; SQ 2012, EURUSD.

22 CHALLET, CHICHEPORTICHE, LALLOUACHE, KASSIBRAKIS

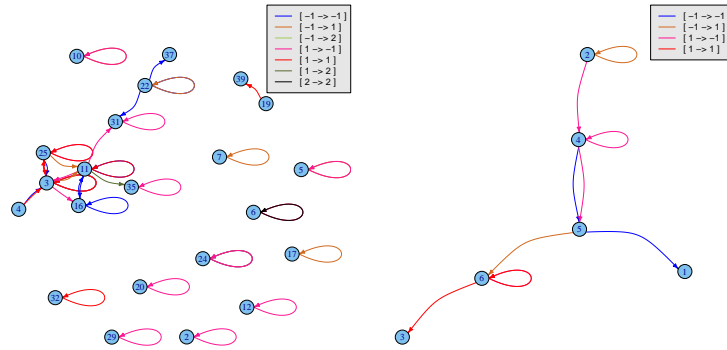


Fig. 5. Examples of lead-lag networks between groups at an hourly scale, for a given date and a calibration window of 50 days (EURUSD, left: SQ, right: LB). 2 labels the neutral state.

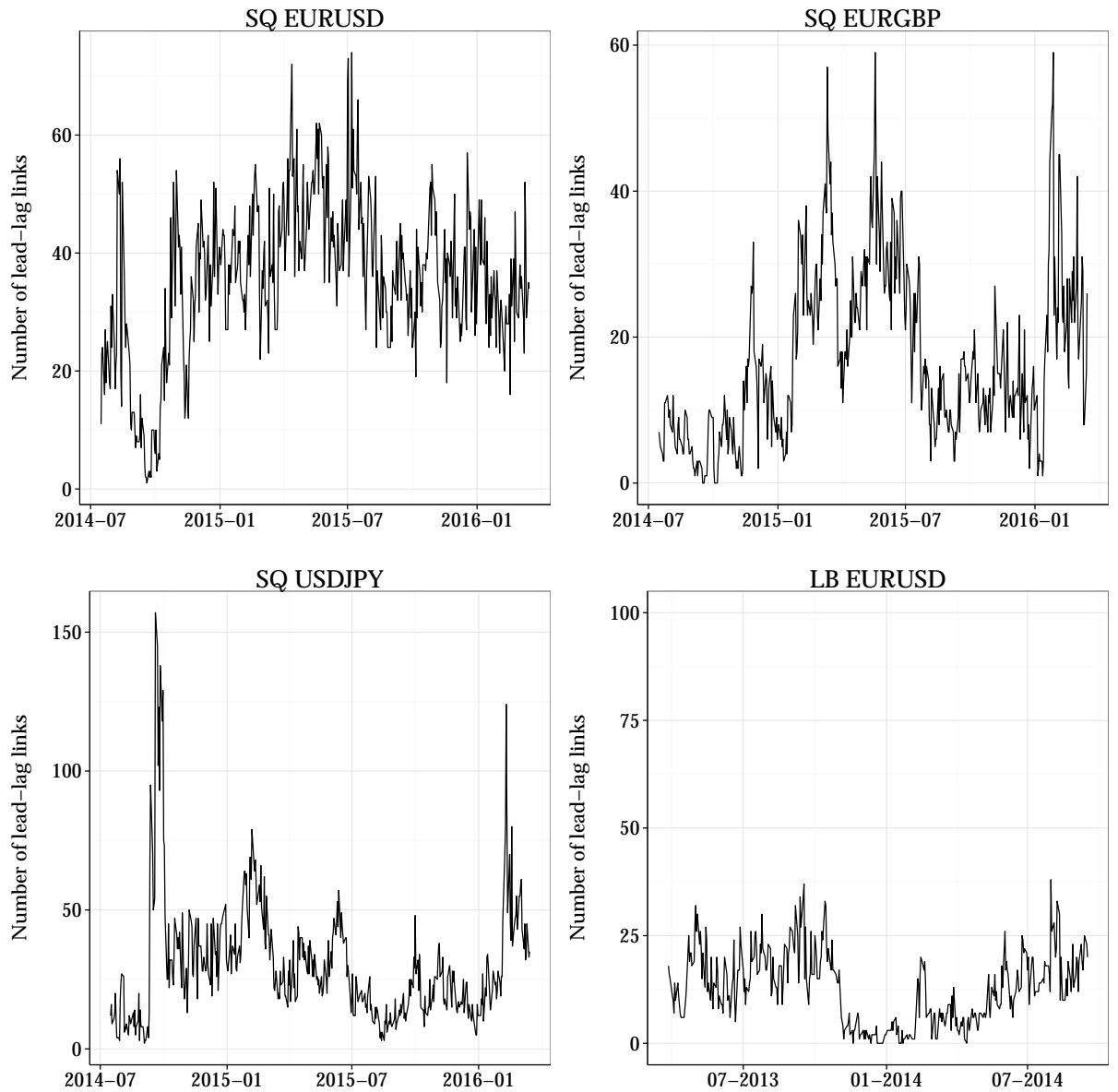


Fig. 6. Lead-lag network of traders: number of links as a function of time. Sliding windows of 45 days of calibration.

24 *CHALLET, CHICHEPORTICHE, LALLOUACHE, KASSIBRAKIS*

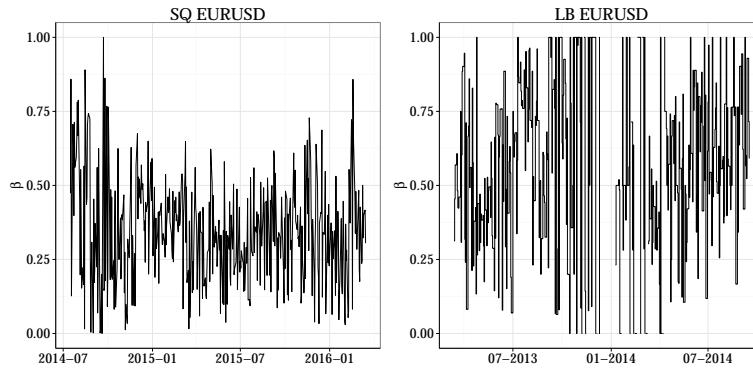


Fig. 7. Trader-trader lead-lag overlap ratio β as a function of time. Same parameters as in Figure 6.

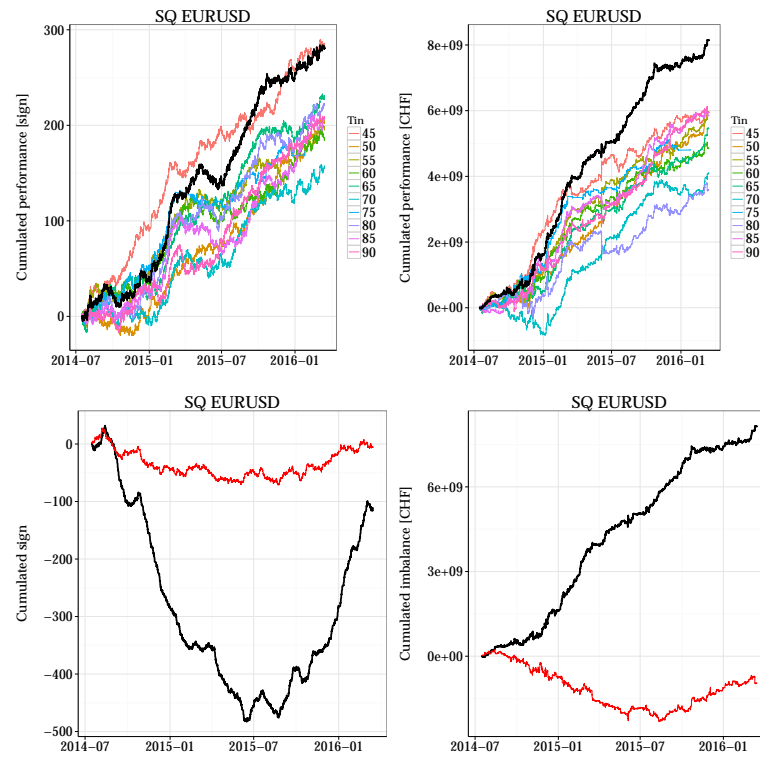


Fig. 8. Out-of-sample performance: cumulated product of the predicted order flow sign and actual sign (upper left), cumulated product of the predicted order flow sign and actual order flow (upper right), cumulated product of the predicted order flow sign and actual order flow, and the cumulated actual flow (lower left), cumulated product of the predicted order flow direction and actual order flow (black line) and cumulated actual order flow (red line); EURUSD, Swissquote. The thick black lines correspond to a majority vote between all calibration window lengths.

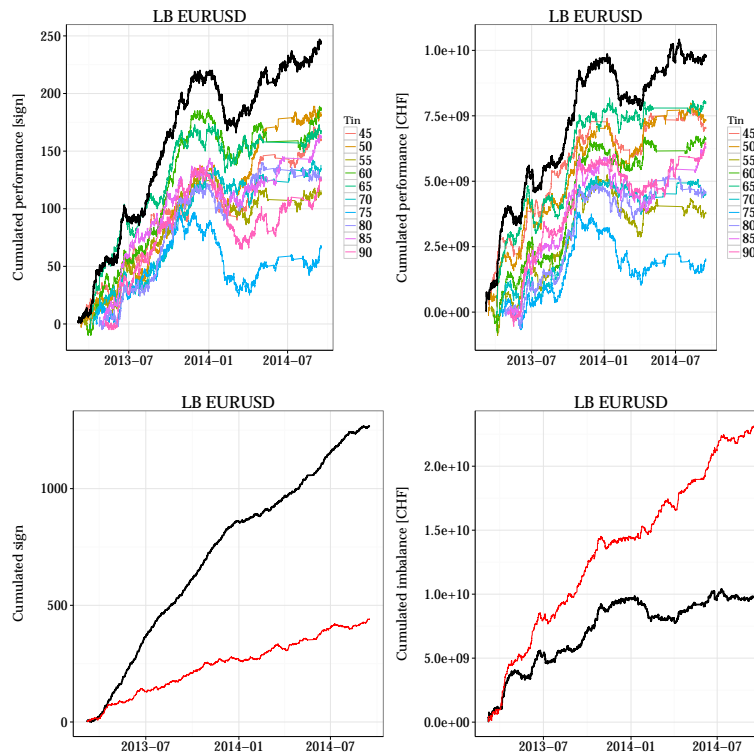


Fig. 9. Out-of-sample performance: cumulated product of the predicted order flow sign and actual sign (upper left), cumulated product of the predicted order flow sign and actual order flow (upper right), cumulated product of the predicted order flow sign and actual order flow, and the cumulated actual flow (lower left), cumulated product of the predicted order flow direction and actual order flow (black line) and cumulated actual order flow (red line); EURUSD, LB. The thick black lines correspond to a majority vote between all calibration window lengths.

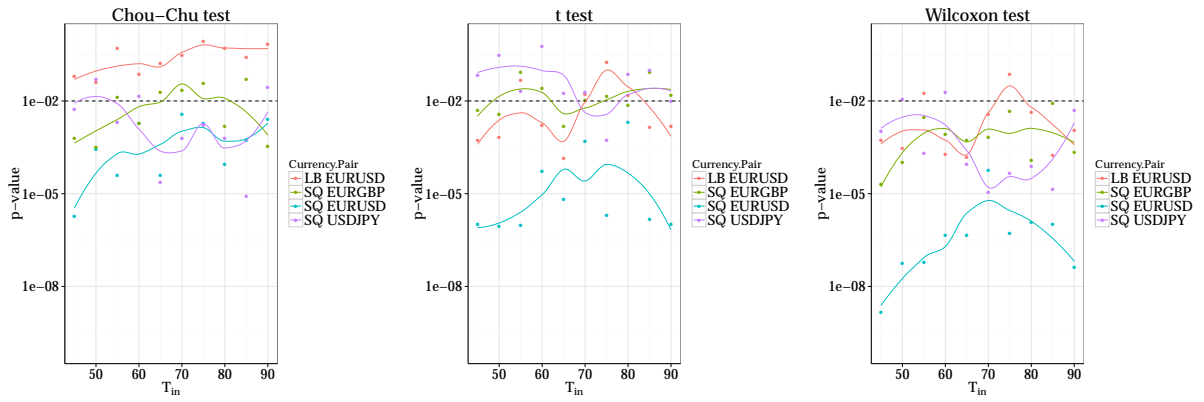


Fig. 10. Tests of the predictive power of the binary prediction (left plot) and two tests of the out-of-sample flow prediction performance. Smoothed curves and dashed lines at $y = 0.01$ are for eye-guidance only.

28 CHALLET, CHICHEPORTICHE, LALLOUACHE, KASSIBRAKIS

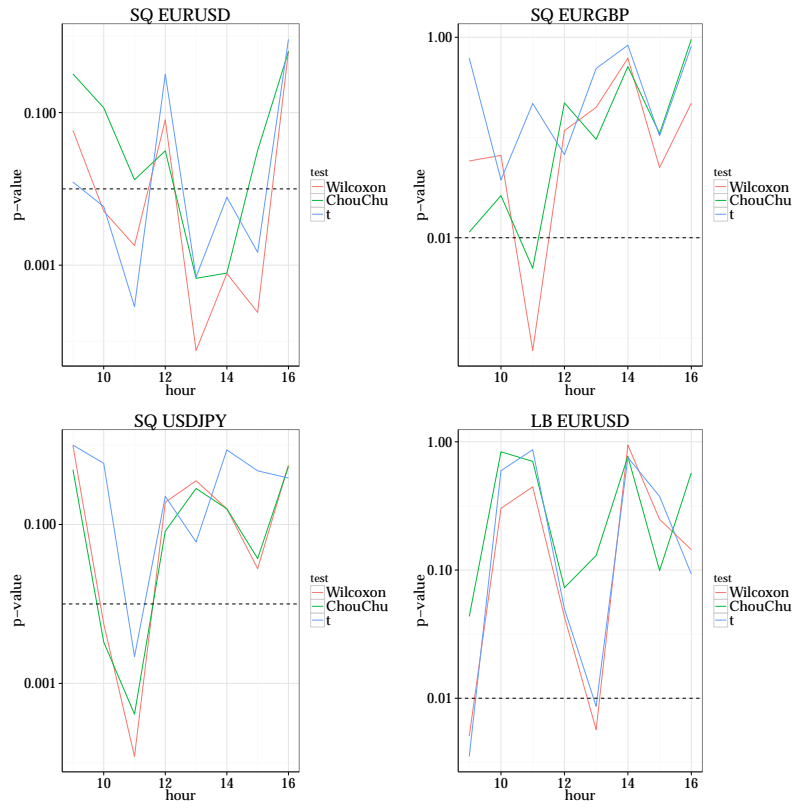


Fig. 11. Test of the predictive power of the binary prediction (Chou-Chu) and of the resulting cumulated predicted imbalance (Wilcoxon and t) as a function of the time of the day.

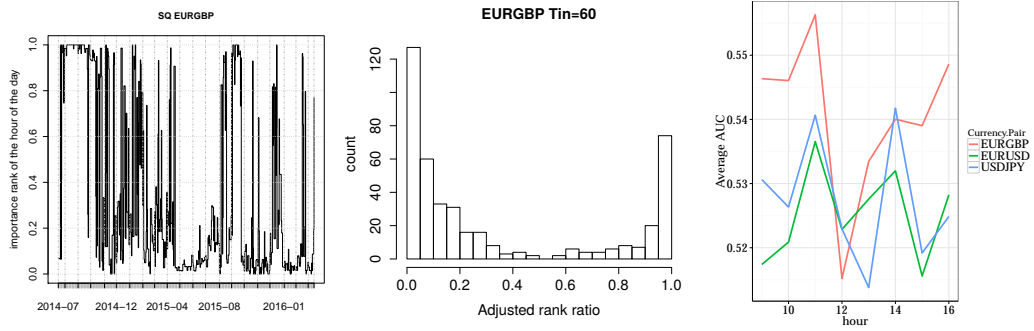


Fig. 12. Adjusted rank ratio of importance of the hour of the days, r_h , for EURGBP as a function of time (left plot) and its histogram (middle plot). The right plot reports the dependence on the Area Under Curve (AUC) of r_h , averaged over all T_{in} , as a function the hour of the day. Dataset: SQ2014-6

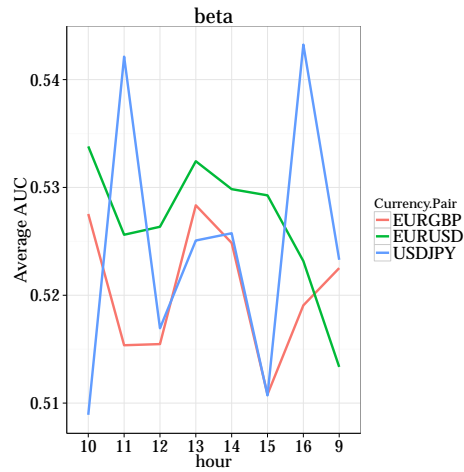


Fig. 13. Area Under Curve (AUC) vs the hour of the day for the trader-trader lead-lag persistence measure β ; SQ 2014-6 dataset.

30 CHALLET, CHICHEPORTICHE, LALLOUACHE, KASSIBRAKIS

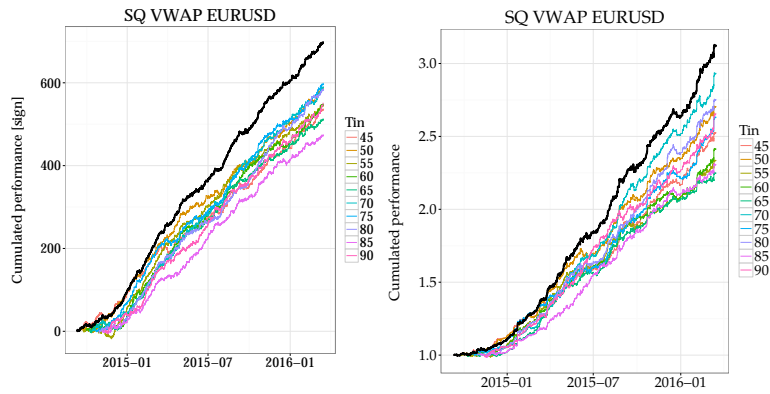


Fig. 14. Out-of-sample performance: cumulated product of the predicted VWAP sign change and actual sign (upper left), cumulated product of the predicted VWAP sign change and actual sign change (upper right); SQ EURUSD. The thick black lines correspond to a majority vote between all calibration window lengths.

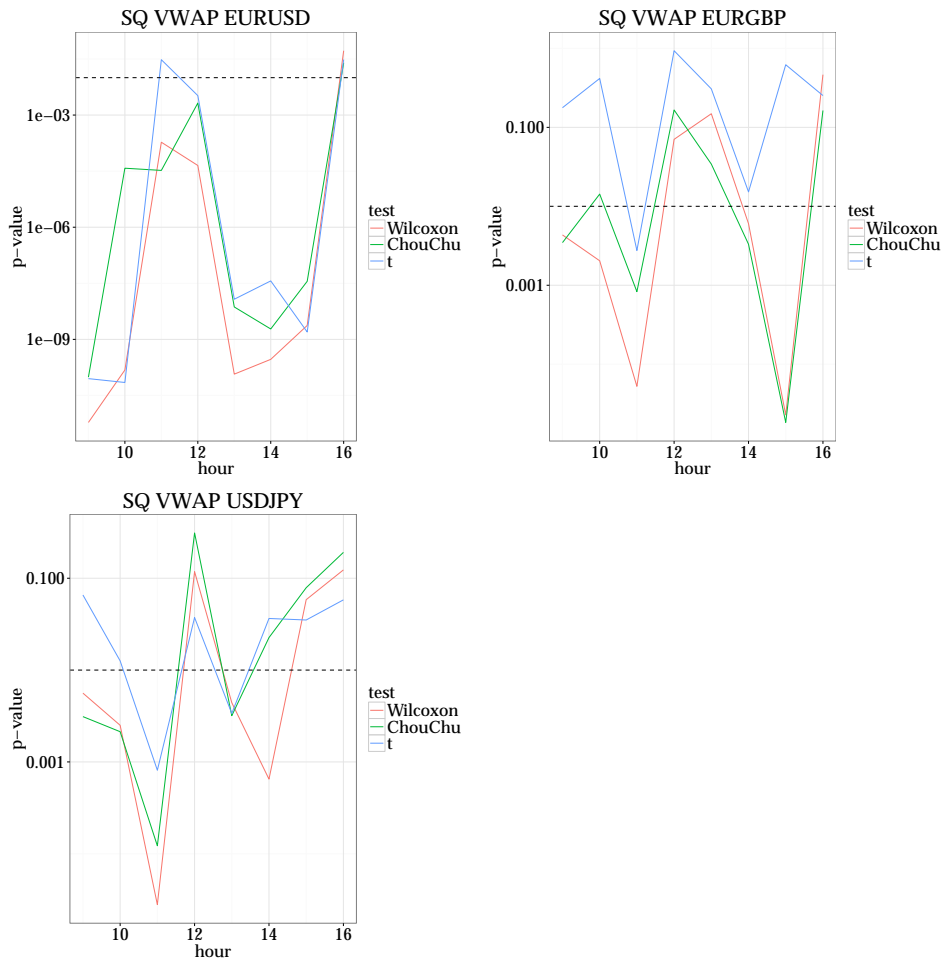


Fig. 15. VWAP change prediction: test of the predictive power of the binary prediction (Chou-Chu) and of the resulting cumulated predicted performance (Wilcoxon and t) as a function of the time of the day; SQ.

32 CHALLET, CHICHEPORTICHE, LALLOUACHE, KASSIBRAKIS

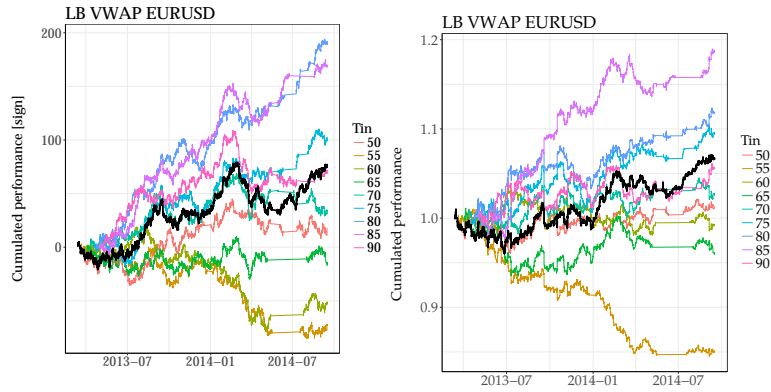


Fig. 16. Out-of-sample performance: cumulated product of the predicted VWAP sign change and actual sign (upper left), cumulated product of the predicted VWAP sign change and actual sign change (upper right); LB EURUSD. The thick black lines correspond to a majority vote between all calibration window lengths.

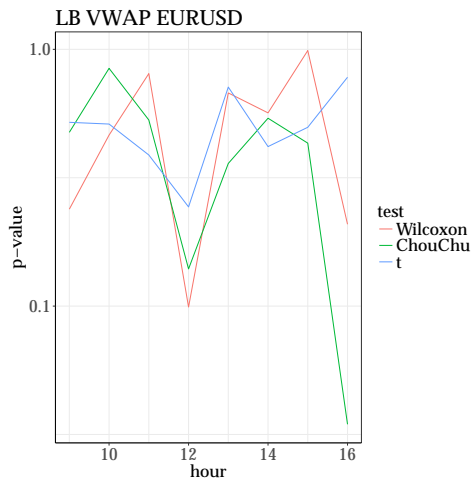


Fig. 17. VWAP change prediction: test of the predictive power of the binary prediction (Chou-Chu) and of the resulting cumulated predicted performance (Wilcoxon and t) as a function of the time of the day; LB, EURUSD.

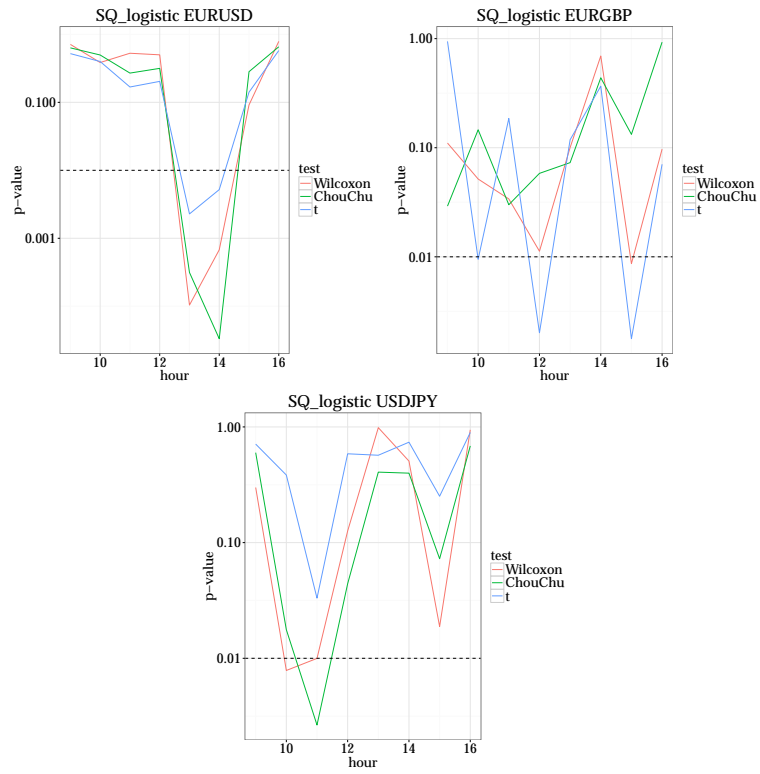


Fig. 18. Hourly statistics of the prediction performance of a logistic regression; SQ2014-6.